testing of the MOS in February and March 1976, there were times when it did not seem possible that the strategy would ever converge and become an operational construct that could function smoothly day after day. Adverse reaction to some of those early problems might have resulted in too little adaptability. However, a concept was worked out by the engineers and scientists, which ameliorated the process, and by the time of the landing the strategy was workable. Since that time, further insights into the process have streamlined the strategy even more.

The most impressive credentials that the Viking MOS can proffer are the extensive changes that have been made in the Viking mission design as a result of the feedback from the scientific data that have been acquired. Most of these changes have been made in a way that is consistent with the strategy. However, and this is an important point, because the strategy has been working so effectively, time and energy have been available to make changes that are scientifically important but cannot be handled as part of regular operational procedure.

A perfect example of a scientifically important late adaptive change occurred after the relay link data from sol 32. At that particular time, the x-ray fluorescence instrument was going through a sequence of discard operations designed to clear its cavity of the first soil sample and to prepare the instrument for the second sample. Since the first sample had been "fines" and the second sample was to be rocks that might have been constructed of different elements, it was of considerable importance that the first sample be removed so that the analysis of the rocks would not be corrupted.

The relay link from sol 32 contained the results of x-ray analyses conducted after each of the first two discard operations. These data indicated that the martian fines were far "stickier" than any test soils that had been used and, more importantly, an extrapolation from these data suggested that the x-ray instrument would still not be very clean at the conclusion of the four discard sequences planned prior to the acquisition of the rock sample. The x-ray team requested that the operating rules be waived to allow a late adaptive uplink that would specify two extra discard operations, bringing the total to six, before the sample acquisition. Complicating their request was the fact that the commands would have to be transmitted on sol 33, 12 hours after the request, when there was not even a normal command load planned.

Through familiarity with the uplink activity, the x-ray team and their engineering support knew the right path to take to have the sequence altered. A few engineering specialists were detailed to construct the command files pending the possible outcome of the decision. The project management weighed the scientific rationale against the engineering risks and decided to prepare the commands. Six discards were made before the new sample was acquired.

Numerous examples similar to the x-ray extra discard request could be cited. At one point there was some slight concern that single-channel counting might be necessary to validate fully the second peak of pyrolytic release on the biology control experiment. It would have required a late adaptive command to implement this change but since the science rationale was overwhelming, the flight operations personnel were marshaled in an overtime mode to prepare the contingency sequences. The commands were not needed, it turned out, but all the work had been completed by the time the data were available to obviate the additional commands.

Although some attention has been focused on those examples where Viking's adaptability was more rapid than that normally provided for in the strategy, most of the time the MOS has met the response requirements. The evolution of both the biology and GCMS instrument strategies has been significantly influenced by the acquired data. The strategy changes are not only in the Viking 1 mission design but also extend to the initial lander sequences for Viking 2. Taking advantage of the early determination of the low amount of argon in the atmosphere, for example, the GCMS team designed an enrichment sequence that would highlight the less abundant gases and increase the accuracy of key isotope ratios. Virtually every investigation has altered its strategy in a similar manner on the basis of early scientific results.

The Viking MOS was designed to be adaptive so that the totality of the Viking scientific contribution would not be limited by those ideas about Mars that were prevalent before beginning the in situ investigations. The exciting and surprising results from Mars, plus the resultant alteration of the experiments to expand upon these results, has proved not only that the MOS design was sound, but also that the time and effort spent in constructing and testing the adaptive operational architecture were justified.

B. GENTRY LEE

Martin Marietta Aerospace, Jet Propulsion Laboratory 264-325, Pasadena, California 91107

Notes

1. The strategy outlined in this paper was developed over a long period and many people made major contributions to it. Among those whose efforts warrant mention by name are O. L. Butler, C. G. Cooley, N. G. Freeman, R. T. Gamber, M. M. Grogan, S. Z. Gunter, J. P. Hardy, H. M. Holt, J. K. Kerekes, D. W. Marquet, J. F. Newcomb, J. D. Porter, D. G. Roos, P. S. Stafford, and H. N. Zeiner. Special thanks go both to the Viking project management, who understood from the beginning that scientific adaptability was the sine qua non of the flight operations, and to the Viking scientists, who saw that the strategy was being developed for them and participated actively in the somewhat painful stages of the design.

2 September 1976

Search for the Viking 2 Landing Site

Abstract. *The search for the landing site of Viking 2 was more extensive than the search for the Viking 1 site. Seven times as much area (4.5 million square kilometers) was examined as for Viking 1. Cydonia (B1) and Capri (C1) sites were examined with the Viking 1 orbiter. The B latitude band (40° to 50°N) was selected before the final midcourse maneuver of Viking 2 because of its high scientific interest (that is, high atmospheric water content, surface temperature, possible near-surface permafrost, and a different geological domain). The Viking 1 orbiter continued photographing the Cydonia (B1) site to search for an area large and smooth enough on which to land (three-sigma ellipse; 100 by 260 kilometers); such an area was not found. The second spacecraft photographed and made infrared measurements in large areas in Arcadia (B2) and Utopia Planitia (B3). Both areas are highly textured, mottled cratered plains with abundant impact craters like Cydonia (B1), but smaller sectors in each area are partially mantled by wind-formed deposits. The thermal inertia, from which the grain size of surface material can be computed, and atmospheric water content were determined from the infrared observations. A region in Utopia Planitia, west of the crater Mie, was selected: the landing took place successfully on 3 September 1976 at 3:58:20 p.m. Pacific Daylight Time, earth received time.*

An earlier report (*1*) described the successful search for the Viking 1 landing site. Even before the successful landing of Viking 1, the Viking 1 orbiter was used to obtain pictures of the Cydonia (B1) and Capri (C1) candidate landing sites, located at 44°N and 5°S (Fig. 1). Typical pictures of the B1 area are shown in Figs. 2 and 3; fractured terrain, craters, and ejecta make these areas unacceptable as a landing site. The original B1 area was therefore rejected.

An alternate site at Capri (C1) at 5°S was photographed but rejected because of the higher scientific interest in the latitude band 40° to 50°N (higher atmospheric water and possible permafrost at the surface). This decision was based on the successful landing of Viking 1 and made with the recognition that less was known about the northern latitude region. Additional areas at B2 (46°N, 110°W) and B3 (46°N, 230°W) were delineated as shown

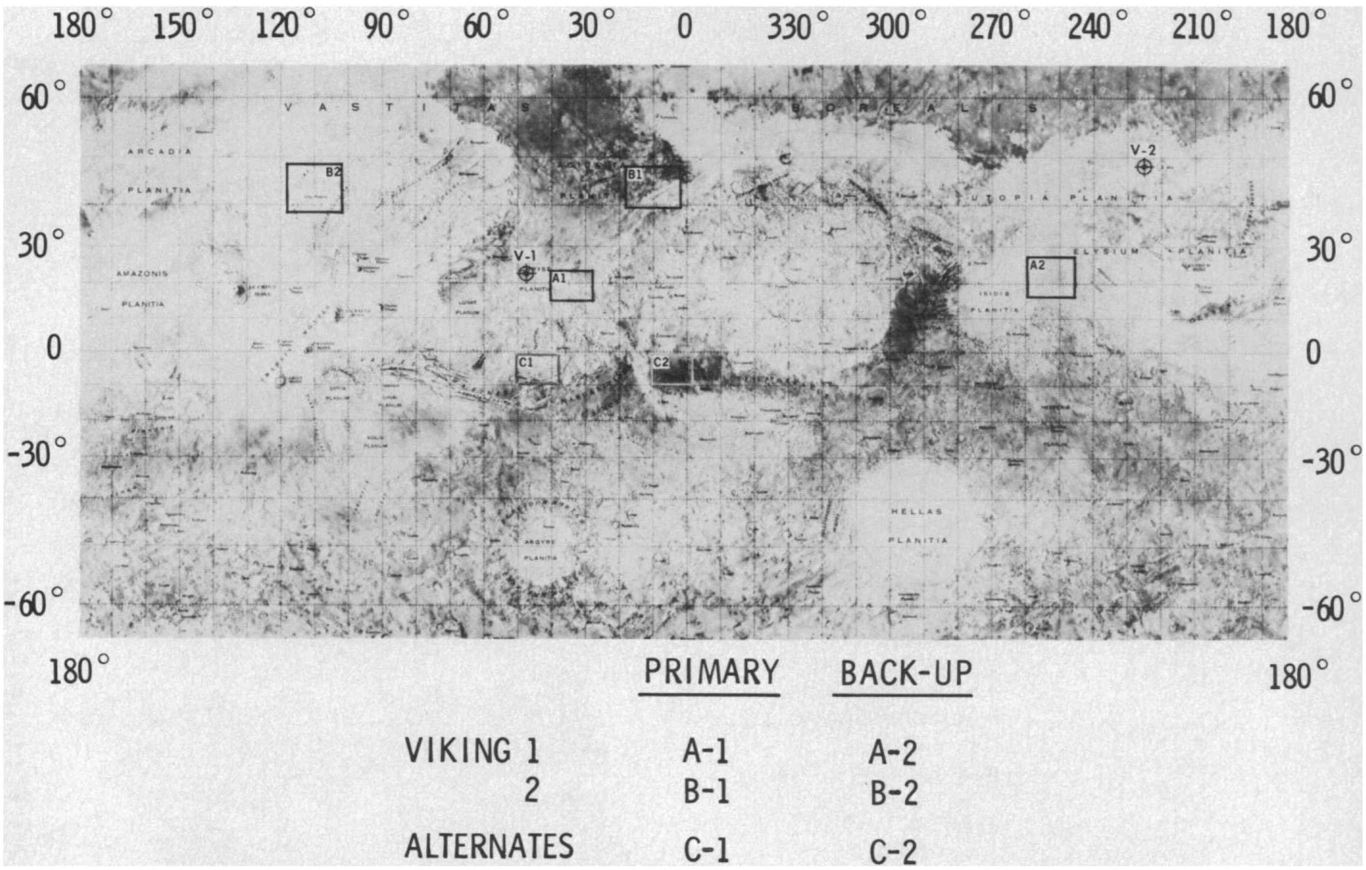

Fig. 1. Viking landing sites.

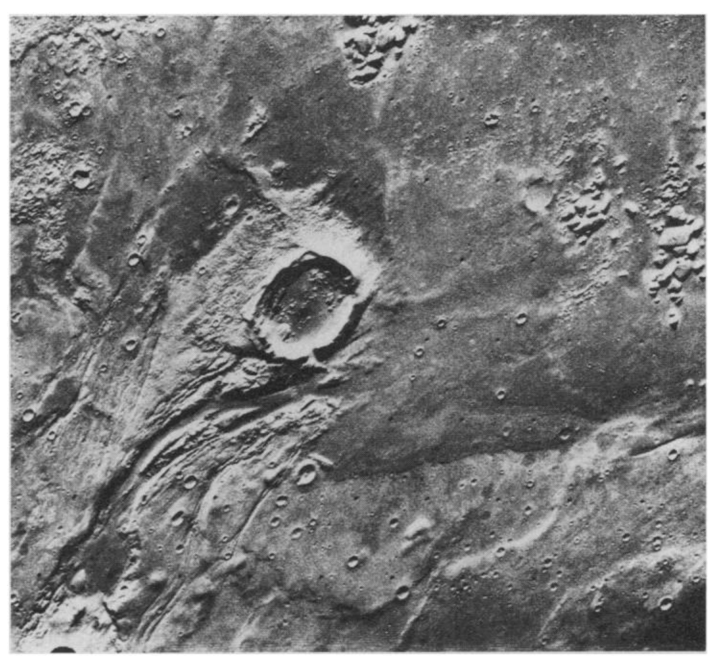

Fig. 2 (left). Polygonal fractures in possible basaltic lava flows in the martian lowlands near the B1 candidate site. Impact craters with ejecta blankets are shown. Secondary craters preserved on a thin wind-deposited mantle stand as small domes with summit craters. Isolated outlines of other rocks protrude through the lavas. Fig. 3 (right). Photograph of plains area in the southeastern part of the B1 area. Stream channels are apparent to the southeast of the impact crater. Many channels are present as far north as 44°N. Stream sapping as well as aeolian deposition is evident in many places in the 40° to 50°N band.

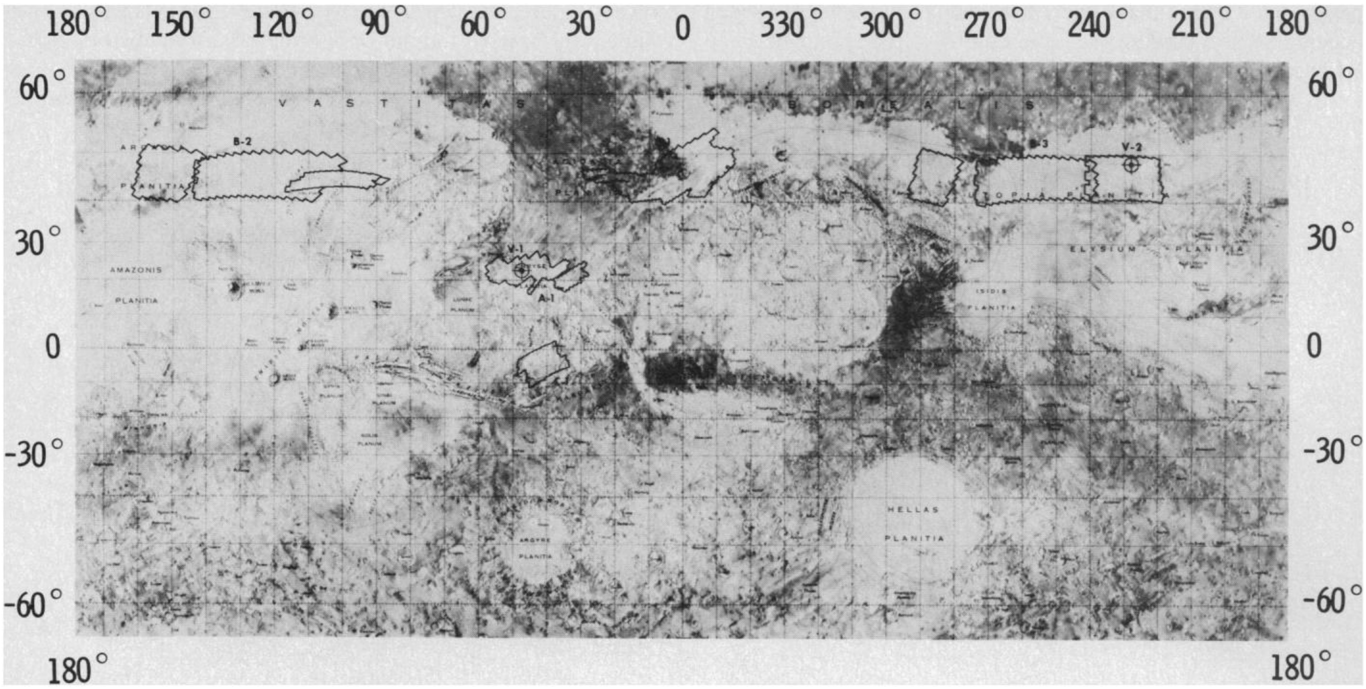

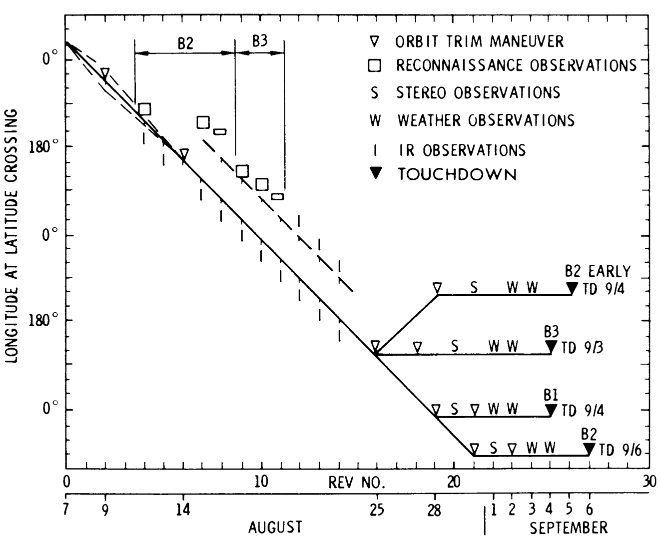

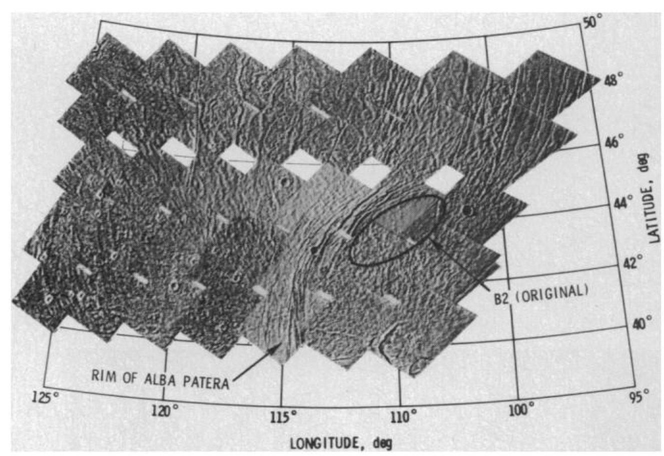

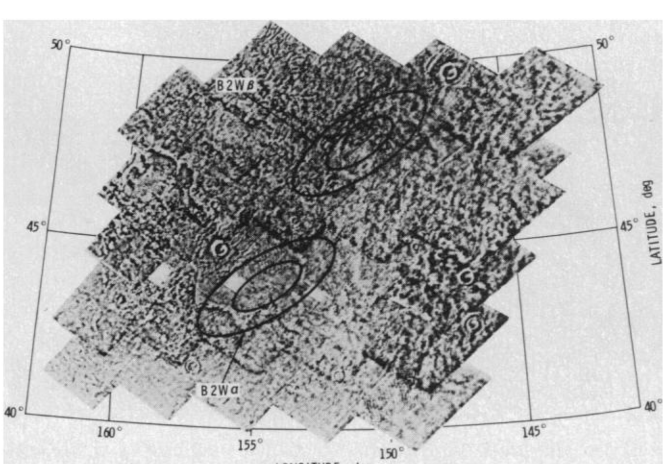

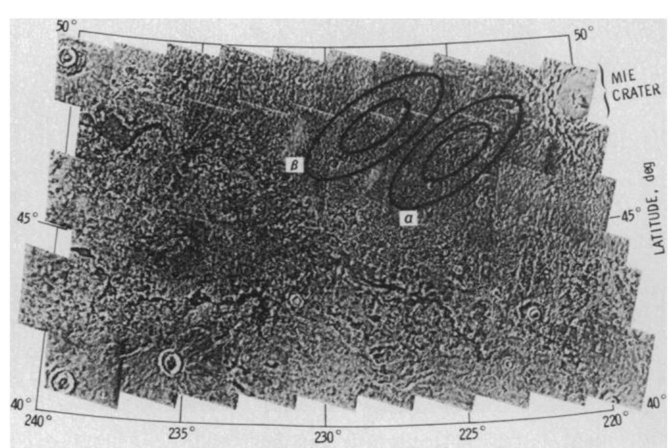

Fig. 4 (top). Viking 1 and Viking 2 photographic coverage for site certification. Fig. 5 (center left). Viking 2 mission strategy. Fig. 6 (center right). Partial B2 mosaic—Alba Patera. Fig. 7 (bottom left). B2W region and candidate sites. Fig. 8 (bottom right). B3E region and candidate sites.

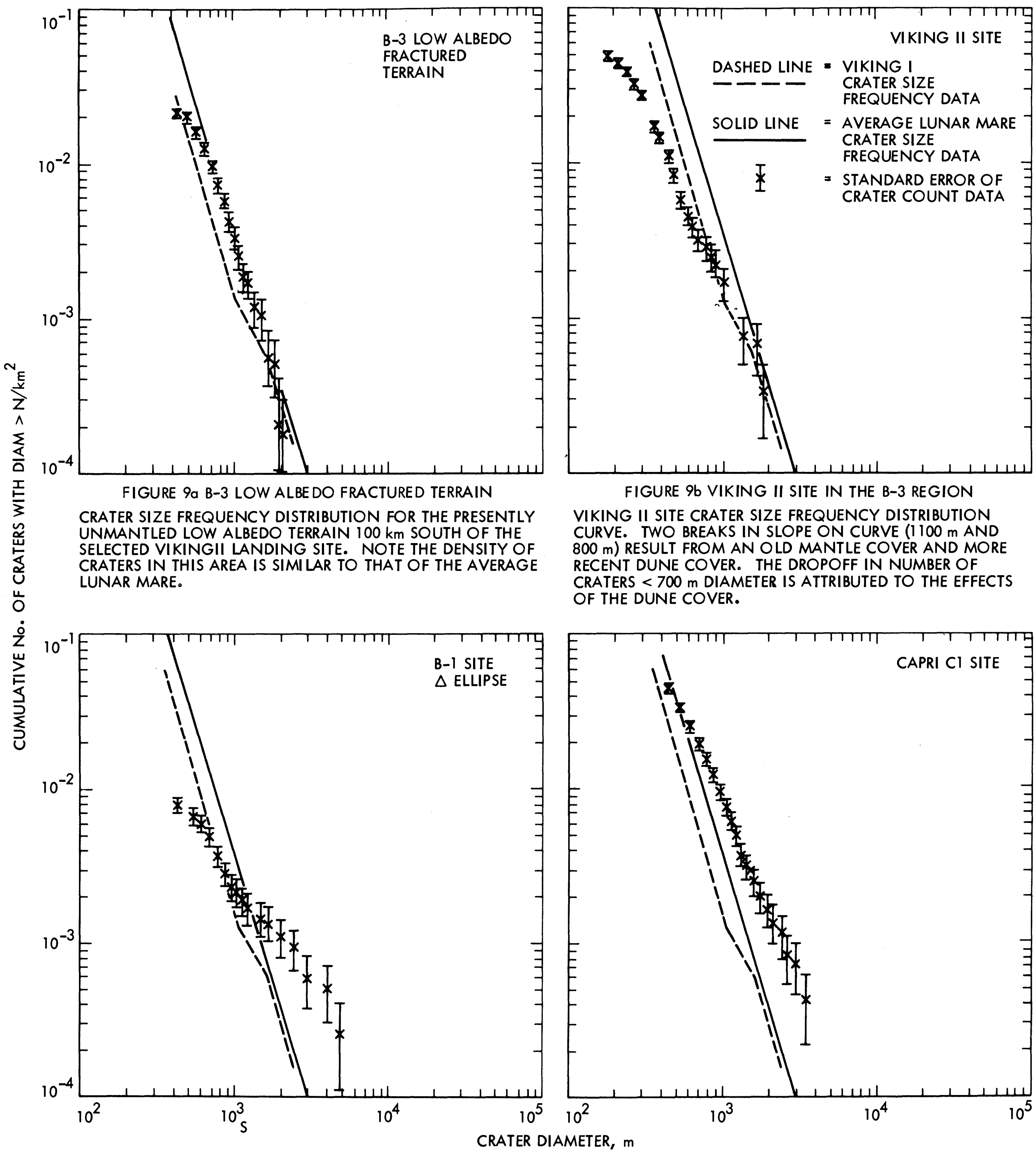

FIGURE 9a B-3 LOW ALBEDO FRACTURED TERRAIN

CRATER SIZE FREQUENCY DISTRIBUTION FOR THE PRESENTLY UNMANTLED LOW ALBEDO TERRAIN 100 km SOUTH OF THE SELECTED VIKINGII LANDING SITE. NOTE THE DENSITY OF CRATERS IN THIS AREA IS SIMILAR TO THAT OF THE AVERAGE LUNAR MARE.

FIGURE 9b VIKING II SITE IN THE B-3 REGION

VIKING II SITE CRATER SIZE FREQUENCY DISTRIBUTION CURVE. TWO BREAKS IN SLOPE ON CURVE (1100 m AND 800 m) RESULT FROM AN OLD MANTLE COVER AND MORE RECENT DUNE COVER. THE DROPOFF IN NUMBER OF CRATERS < 700 m DIAMETER IS ATTRIBUTED TO THE EFFECTS OF THE DUNE COVER.

FIGURE 9c B-1 SITE Δ ELLIPSE

CRATER SIZE FREQUENCY DISTRIBUTION CURVE FOR A THICKLY MANTLED REGION IN THE B-1 VIKING II CANDIDATE LANDING SITE. THIS CURVE SHOWS THAT THE LARGER CRATERS (> 2000 m DIAMETER) IN THIS REGION HAVE A DISTRIBUTION LIKE THAT OF THE C1 CAPRI SITE (AN OLD HEAVILY CRATERED SURFACE) AND THE SMALL CRATER POPULATION IS LIKE THAT OF THE VIKING I LANDING SITE. THIS IS INTERPRETED TO MEAN THAT PRE-MANTLE CRATERS SMALLER THAN ~ 200 m DIAMETER ARE BEING BURIED BY THE MANTLE.

FIGURE 9d CAPRI C1 CANDIDATE SITE

CRATER SIZE FREQUENCY DISTRIBUTION CURVE FOR CAPRI, VIKING I CANDIDATE LANDING SITE IN THE MARTIAN EQUATORIAL REGION (-7°S, 43°). CAPRI IS THE MOST CRATERED (OLDEST) OF THE VIKING CANDIDATE SITES AND WAS CHOSEN ON THE BASIS OF EARTH-BASED RADAR DATA AS BEING QUITE SMOOTH AT THE VIKING SPACECRAFT SCALE.

Fig. 9. Crater frequency counts.

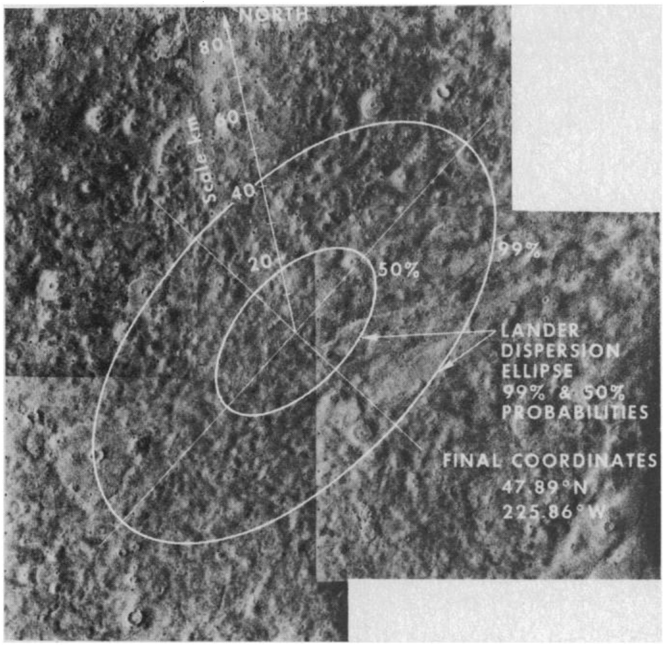

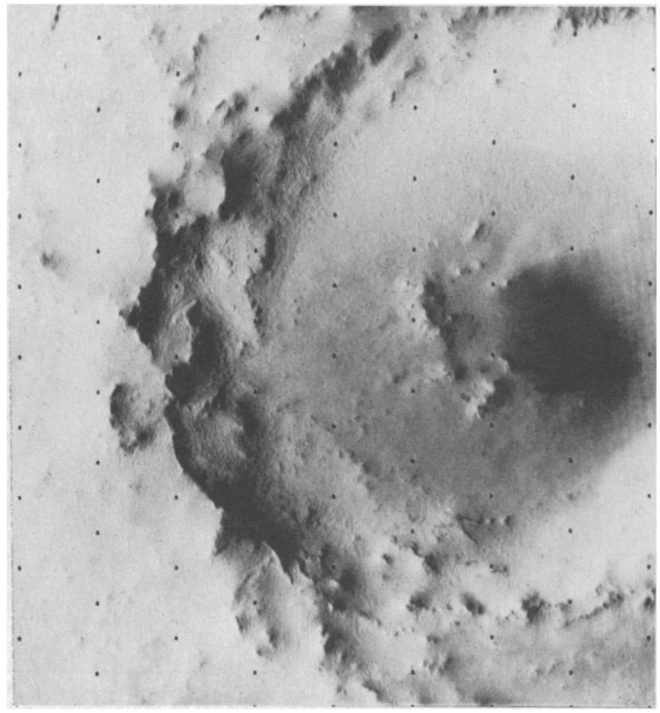

Fig. 10 (left). Detail of final Viking 2 landing site. Fig. 11 (right). Crater Mie east of landing site. The crater Mie is about 100 km in diameter and lies 200 km east of the landing site. It is similar to the impact crater Copernicus on the moon with its complex central peak and rugged rim. Dunes about 1 km from crest to crest mantle the west wall of the crater. These dunes are larger and clearer than the dunes in the site. Wind-eroded pits lie on the floor of the crater. Thus, both deposition and erosion must have occurred in this crater; it is presumed that they must both have occurred in the landing site also.

in Fig. 4, based on interpretations of the Mariner 9 pictures, which indicated the existence of a mantling aeolian deposit at these regions.

At about the time of the first Viking landing on 20 July 1976, the strategy for the second spacecraft was reviewed and modified to provide coverage of the three regions delineated in the latitude band 40° to 50°N (Fig. 5). The Viking 1 orbiter continued to observe to the east of the B1 site, searching for a smooth mantled area. Orbit trim maneuvers were planned to accommodate landing anywhere within the B1, B2, or B3 regions. By 21 August, rev 13, it was necessary to decide whether a trim would be made on 25 August, rev 16, to go to B3 to land on 3 September or to go to B1 or B2, with a landing on 4 or 6 September, respectively. The strategy was planned to permit most of the site observations to be done after the Viking 2 orbit had been adjusted on rev 6 to minimize the effects of orbit dispersions on the observation geometry. One set of pictures was planned on rev 4 before the trim orbit had been attained to permit coverage of the area to the east of Alba Patera; after rev 6 that area would be in the dark and not observable. An important feature of the strategy was the observations of the B2 and B3 regions when the spacecraft passed over the target latitudes southbound, at 0° to 30° from the afternoon terminator and at slant ranges of more than 3000 km. Infrared observations to determine atmospheric water content and thermal inertia (therefore surface grain size) of the B1, B2, and B3 regions were designed for the northbound crossing of the target latitude at ranges of 1500 km at various times of the day.

Early results and changes. As a result of continued observation of the extended B1 region by Viking 1, small areas of aeolian mantle that blanket craters, ejecta, and polygonally fractured ground were identified at the east end of the B1 site. A complex history of aeolian deposition interleaved with erosion stripping is recorded. In some cases secondary crater clusters pepper the small plains. In other areas, stripping of the uppermost aeolian mantle has occurred, leaving secondary craters protruding as hummocks where crater ejecta has inhibited stripping. In any case, the small areas of aeolian mantle were not large enough to locate an ellipse in, and the entire B1 region was rejected.

Coverage of Alba Patera in B2 on revs 4 and 7 raised, and then dashed, hopes that it would prove to be a suitable landing site. The rev 4 photo calibration sequence indicated a possible site on the top of Alba Patera, but rev 7 results (Fig. 6) indicated that under suitable illumination the area appeared rough, being covered by textured lava flows. In addition, the atmospheric water content was much lower on the top of the volcanic plateau (*2*). Alba Patera was therefore abandoned as a candidate landing site.

As a consequence of the negative results for the B1 and B2 regions, and the increasingly obvious operational difficulties in maintaining the multiple options in the mission strategy, the decision was made on 16 August to proceed with one main option, B3, where no data had yet been obtained. All observations planned through rev 15 would be taken and processed as planned; however, no specific operational planning would be done for the B1 and B2 options. Data on B3 from revs 9 and 10 were obtained, and close inspection yielded "possible" sites with "acceptable" hazards. Continuing analysis of the B2 region defined two other possible sites with acceptable hazards.

On 21 August a formal review was held of the candidate sites, two in each of the B2 west and B3 east regions (Figs. 7 and 8). In defining these candidate ellipses, it was necessary to consider new hazard criteria. In the analysis of Viking 1 sites, individual rock units were mapped and put in a time sequence; in the Viking 2 analyses, hazards were defined as crater ejecta and steep slopes, and areas subject to different surface processes (stripping, mantling, and texturing) were mapped to determine favorable areas.

From the picture coverage, there appeared to be areas covered with a texture that was tentatively identified as dunes in both the B2 and B3 sites. The dunes in B2 appeared to be bigger and more identifiably thicker than those in B3. This was counterbalanced by the muting at B3 due to a pitted aeolian mantle in addition to the "dunes." At B3, the terrain changed from stripped to muted from south to north—cracks became shallower, albedo markings disappeared, and craters were less abundant. The B2 pictures contained image defects and clouds, so although craters were visible, some photo interpreters felt more cautious about the areal extent of dunes at B2 than at B3. Modifications to the crater frequency counts (*3*) appeared at diameters of several hundred meters, indicating mantling by aeolian materials in the northeastern part of the B3 region (Fig. 9b). This is confirmed by the dunes and pits within the crater Mie. It was believed that this diminution in cratering extended down to the scale of the lander.

The portion of the B3 site in which the landing site lies has a lower crater count because of the mantling by the dune material (compare Fig. 9a and Fig. 9b). A similar decrease in craters is evident in the sand dune–covered part of the western B2 site. In the southern and western part of B3, the stripped area (fractured terrain) shows a much higher crater count than the dune-covered area. A similar increase in craters is apparent in the B1 site (Fig. 9c), where the surface is also stripped. The Capri site (Fig. 9d) in the higher older cratered terrain shows a large increase in crater frequency too.

Some observers (including H.M.) felt that the craters and blocks in the ejecta

Fig. 12 (upper left). Polygonally fractured plains—these probably are lava flows with cooling cracks. The cracks also have been interpreted as thermally induced patterned ground. The fractures are partially filled with wind-blown material that is thinner and more uniform than dune material farther east. Fig. 13 (upper right). Unnamed stream channel that extends 600 km to the south toward Elysium Montes. A tributary starts at the right of the picture in a "box canyon" that possibly is due to spring sapping. Fig. 14 (lower right). Impact crater southwest of landing site. The ejecta has been eroded by the wind so it has negative relief. It may be that the ejecta here was fine-grained enough to be eroded in this manner. The adjacent lava flows are etched out by the stripping action of the wind too.

in B2, being smaller than those in B3, were better covered by the bigger dunes apparent in the B2 pictures, and that the smaller dunes in B3 might not cover the ejecta from the larger craters there as well. Site B3 was favored by still others independent of the dune argument since it appeared to them that B3 was smoothed by uniform mantling.

In the B sites, where dunes and aeolian mantle were observed, an attempt was made to estimate thickness of cover based on dune spacing and dune slopes. The minimum thickness was estimated as being adequate to cover small crater ejecta. Estimating impact crater ejecta block size at two crater diameters from the crater Mie (100 km in diameter) was difficult. The estimated 10-m block size was based on ejecta sizes measured in the Surveyor 7 landing site and Apollo 15, Apollo 16, and Apollo 17 high-resolution photographs. The block populations depend on the number of small craters below the resolution limit that may excavate blocks from below the wind-laid mantle and the number exposed by deflation. Slopes were deemed as acceptable based on Earth analogs, except on the inner margins of craters.

The infrared thermal mapper results for the B2 region indicated low thermal inertia and large amounts of fines (*4*). No data were available for the specific candidate ellipses. The thermal inertia at B3 was determined to be approximately similar to that at the Viking 1 site; the required noon coverage was not available (*4*).

Observations showed more atmospheric water at B2 than at B3 (*2*). There was a greater diurnal variation in water content at B2 and it had an assumed 10° warmer surface temperature, although no data were available at the site.

These factors were carefully weighed; and the B3 site was selected for the following reasons.

1) *Safety*. It appears that B3 is adequately mantled, muted, and filled. Site B2 may be as good, but the seeing due to clouds and imaging quality diminishes confidence in the coverage. Site B3 appears more homogeneous throughout the area of the 99 percent ellipse.

2) *Science*. There is a small distinction between the sites. The warmer temperature at B2 is in its favor. The water content difference was not deemed significant. The most significant scientific distinction had already been realized when the northern latitude band was selected.

3) *Operations*. Implementation is straightforward at B3. The additional data analysis and acquisition required to land at any other site could result in a landing delay and significant additional operational complexity. Acceptance of this additional complexity was not justified, based on the B3 assessment cited above.

Subsequently, the B3 α and β ellipses (Fig. 8) were coalesced into one with preliminary coordinates of 48°N, 226°W. Final coordinates (47.89°N, 225.86°W) were selected on 30 August after review of the rev 20 stereoscopic coverage. Detailed mosaic of the landing site with the lander dispersion ellipse is given in Fig. 10.

The crater Mie east of the landing point is covered with larger dunes and deflation hollows (Fig. 11), and the polygonally fractured lava flows west of the site (Fig. 12) are covered with a thin mantle of wind-blown material that partially fills the fractures. At the south end of the B3 region, a large channel (Fig. 13) dissects and crosses the area, extending 600 km to the south toward the Elysium volcanoes. Some of the large craters (Fig. 14) are extensively modified by wind erosion, possible water sapping, and dissection, so that their ejecta blankets are etched out in negative relief. The area is thus partially mantled by aeolian material in the north, where the landing site is located, and stripped in the south. The crater counts previously cited confirm this interpretation.

The conclusion of the search for the Viking 2 site was the selection of the B3 site in Utopia Planitia. The landing was successfully accomplished at 3:58:20 p.m. P.D.T., earth received time, on 3 September 1976.

Studies are under way to compare the actual conditions encountered at both the Viking 1 and Viking 2 landing sites with those expected on the basis of the prelanding observations. These results will be reported on when completed. Tentatively, Viking 2 rests in a deflation hollow.

H. MASURSKY
U.S. Geological Survey, Flagstaff, Arizona 86001
N. L. CRABILL
NASA Langley Research Center, Hampton, Virginia 23665

References and Notes

1. H. Masursky and N. L. Crabill, *Science* **193**, 809 (1976).
2. C. B. Farmer, personal communication.
3. G. Schaber, J. Boyce, A. Dial, M. Strobell, and G. Stewart provided near-real-time crater counting and analyses for these and many other locations.
4. H. Kieffer, personal communication.
5. The Viking 2 site certification effort was a team effort as it was for the Viking 1, except that infrared observations rather than radar data were used in conjunction with images to evaluate the sites. H. H. Kieffer and his associates reduced infrared thermal mapper data and made them available in near real time to help in site evaluation. C. B. Farmer and his team similarly reduced the Mars atmospheric water data very expeditiously. Hazard analyses were done by J. A. Cutts, K. W. Farrell, L. Crumpler, T. Spudis, and E. Theilig. Geological and terrain analyses were performed by J. E. Guest, R. Greeley, G. Schaber, J. Boyce, J. A. Cutts, K. W. Farrell, M. H. Carr, and L. Soderblom. Image data processing proceeded through a complicated chain with the help of R. Johansen, M. Martin, and associates at the Mission and Test Imaging System Facility; G. Traver and associates at the Mission and Test Photoprocessing System; R. Ruiz and associates at the Image Processing Laboratory; J. Hewitt and associates at the JPL photo laboratory; and R. Tyner and W. Sowers (who made photographic mosaics as fast as these images were delivered). L. B. Garrett and others organized this image processing system; and D. Roos monitored its day-to-day implementation. Thanks are also due to M. J. Alazard, D. L. Anderson, G. A. Briggs, D. M. Davies, J. D. Goodlette, R. Hargraves, S. L. Hess, L. Kingsland, T. Z. Martin, W. H. Michael, H. J. Moore, II, E. C. Morris, T. A. Mutch, F. T. Nicholson, W. J. O'Neil, T. Owen, F. D. Palluconi, J. D. Porter, R. J. Reichert, C. Sagan, R. W. Sjostrom, B. A. Smith, C. W. Snyder, G. A. Soffen, T. E. Thorpe, P. Toulmin III, E. D. Vogt, and the rest of the Viking Flight Team at Jet Propulsion Laboratory and the U.S. Geological Survey at Flagstaff. As before, J. S. Martin, Jr., A. T. Young, and B. G. Lee provided a ready hand at the Viking tiller.

2 September 1976

Isotopic Composition of the Martian Atmosphere

Abstract. *Results from the neutral mass spectrometer carried on the aeroshell of Viking 1 show evidence for NO in the upper atmosphere of Mars and indicate that the isotopic composition of carbon and oxygen is similar to that of Earth. Mars is enriched in* ^{15}N *relative to Earth by about 75 percent, a consequence of escape that implies an initial abundance of nitrogen equivalent to a partial pressure of at least 2 millibars. The initial abundance of oxygen present either as* CO_2 *or* H_2O *must be equivalent to an exchangeable atmospheric pressure of at least 2 bars in order to inhibit escape-related enrichment of* ^{18}O.

Viking 1, which landed on Mars on 20 July 1976, included as part of its scientific payload a mass spectrometer designed to measure properties of the neutral atmosphere between about 100 and 200 km during the descent of the spacecraft to the planet's surface (*1*). A preliminary account of the results has been published (*2*). The martian atmosphere consists mainly of CO_2, with traces of N_2, Ar, O_2, CO, and O. The relative abundances of oxygen and carbon isotopes in the mar-